

## Study on Double-Mode Miniature Cantilever-Type Ultrasonic Motor using Lead-free Multilayer Piezoelectric Ceramics

非鉛積層圧電セラミックスを用いた屈曲2重モード小型片持ちはりモータの研究

Yutaka Doshida<sup>1†</sup>, Hiroyuki Shimizu<sup>1</sup>, Taisei Irieda<sup>1</sup>, Hideki Tamura<sup>2</sup>, Yoshiro Tomikawa<sup>2</sup>, and Seiji Hirose (<sup>1</sup>Taiyo Yuden Co., Ltd., <sup>2</sup>Yamagata University)  
土信田豊<sup>1‡</sup>, 清水寛之<sup>1</sup>, 入枝泰成<sup>1</sup>, 田村英樹<sup>2</sup>, 富川義朗<sup>2</sup>, 広瀬精二<sup>2</sup>(<sup>1</sup>太陽誘電㈱, <sup>2</sup>山形大学)

### 1. Introduction

There is a great demand for microactuators to miniaturize the optical control module in mobile gadgets. Piezoelectric actuators have been partly put to practical use and many studies on ultrasonic micromotors have been carried out. Currently, these piezoelectric actuators are made almost always using PZT ceramics. The actuators using lead-free piezoelectric ceramics are strongly desired from the viewpoint of environment protection. As pioneering work, we succeeded in realizing a double-mode miniature cantilever-type ultrasonic motor using lead-free multilayer piezoelectric ceramics (MLPC) of  $(\text{Sr,Ca})_2\text{NaNb}_5\text{O}_{15}$  (SCNN).<sup>1</sup> In particular, by using an array-type multilayer piezoelectric ceramics (A-MLPC) of SCNN as shown in **Fig. 1**, the lead-free motor was able to rotate by a lithium-ion cell used in the mobile equipment without an amplifier circuit.<sup>2</sup> The driving properties of the lead-free motor were the almost same as those of PZT motor.<sup>1,2</sup> In this study, we discussed how to design the cantilever-type ultrasonic motor, and fabricated a torque-oriented motor, and then investigated the properties of driving.

### 2. Motor design

The structure of A-MLPC and the views of the stator vibrator and the motor are shown in **Fig. 1**. A-MLPC integrated four pieces of MLPC. The motor can rotate by the first-bending-vibration-mode rotation of the stator vibrator oscillated thickness vibration of two pairs of MLPC arranged diagonally in A-MLPC.

To understand the design rule of the cantilever-type motor, the cantilever dimensions dependence of motor characteristics was simulated by the finite element method (FEM). **Table I** shows the dimensions of the stator vibrator for control parameters. The motor characteristics were evaluated from the resonance frequency  $f_0$ , the electromechanical coupling coefficient  $k_{vn}$  of the

stator vibrator, the maximum revolution speed  $\Omega_0$ , and the maximum torque  $T_0$ .  $\Omega_0$  was calculated from the vibration velocity of the vampeplate for the stator vibrator.  $T_0$  was estimated from the thrust  $F_0$  of the vampeplate.  $F_0$  can be calculated by the relationship during the displacement  $u$  of the vampeplate and the preload to the vampeplate. **Figure 2** shows equivalent circuit of the stator vibrator and the relational expressions, and the schematics of the stator vibrator by FEM are shown in **Fig. 3**.

**Figure 4** shows  $h_s$  dependence of  $\Omega_0$  and  $T_0$ . Those values were indicated in the ratio to the value with the basic sizes as shown in **Table I**. The measured values were almost corresponded to the simulation values. Those have the peak values, respectively. The relationships among  $\Omega_0$ ,  $T_0$ , and  $r_v$  are shown in **Fig. 5**.  $\Omega_0$  decreased with increasing  $r_v$ . On the other hand,  $T_0$  increased linearly with  $r_v$ . It shows the motor properties can be designed from the revolution-speed-oriented motor to the torque-oriented one by selecting of  $r_v$ .

### 3. Motor characterization

At previous study, we selected the basic sizes with a balance between the revolution speed and the torque.<sup>1,2</sup> In this study, we designed the torque-oriented motor more by selecting the dimensions of the cantilever. **Figure 6** shows the overviews of the motor with a CD-R shaped rotor and a stator vibrator using A-MLPC of SCNN. By the increasing the torque, the motor started to rotate at  $6 V_{p-p}$  and rotated at 20 rpm by  $10 V_{p-p}$ . As the result, we developed the torque-oriented motor. The motor properties have been evaluated.

### References

1. Y. Doshida, S. Kishimoto, K. Ishii, H. Kishi, H. Tamura, Y. Tomikawa, and S. Hirose: Jpn. J. Appl. Phys. **46** (2007) 4921.
2. Y. Doshida, S. Kishimoto, T. Irieda, H. Tamura, Y. Tomikawa, and S. Hirose: Jpn. J. Appl. Phys. **47** (2008) 4242.

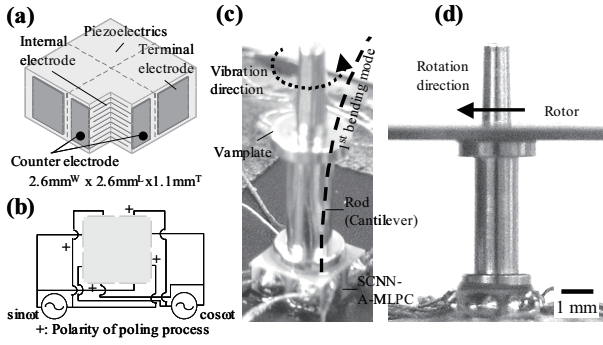


Fig. 1. Cantilever-type ultrasonic motor using A-MLPC of SCNN: (a) structure of A-MLPC, (b) wire diagram of A-MLPC, (c) overview of stator vibrator, and (d) side view of motor.

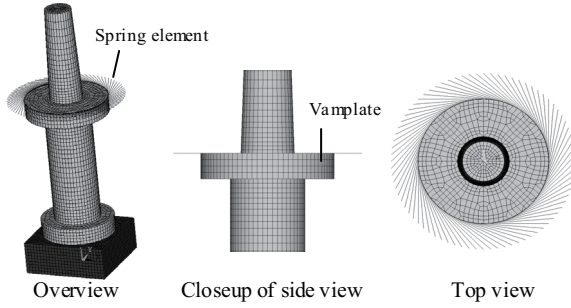


Fig. 3. Schematic views of stator vibrator by FEM.

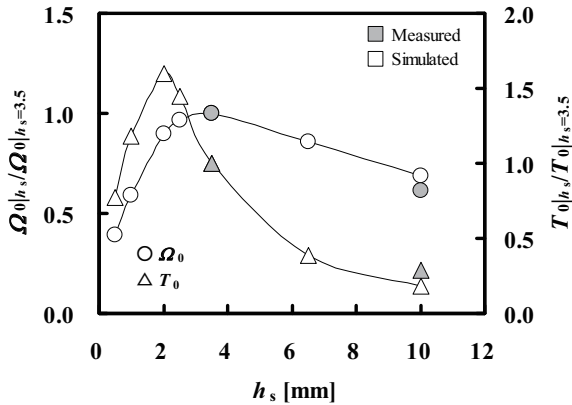
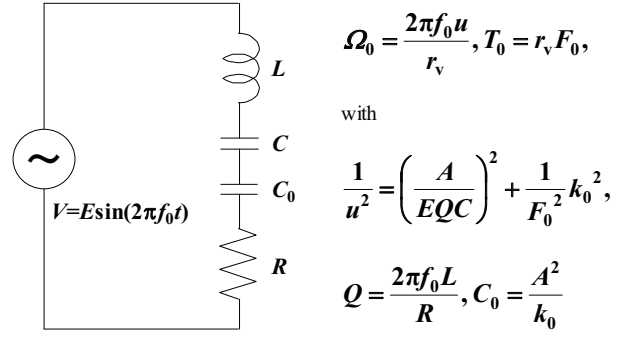


Fig. 4.  $h_s$  dependence of revolution speed and torque for motor.

Table I. Dimensions of cantilever-type stator vibrator.

|               |       | (mm) * |            |
|---------------|-------|--------|------------|
| Cantilever    | $h_u$ | $0.5$  | $3-4$      |
|               | $h_s$ | $0.5$  | $3.5-10$   |
|               | $t_v$ | $0.1$  | $0.5-1$    |
|               | $t_b$ | $0.1$  | $0.5-1$    |
|               | $r_s$ | $0.4$  | $0.7-2.5$  |
|               | $r_v$ | $0.7$  | $1.25-2.5$ |
| Piezo element | $r_b$ | $0.7$  | $1.1-2$    |
|               | $w$   | $1$    | $2.5-4$    |
|               | $t_s$ | $0.2$  | $1-2$      |

\* Underlined parts mean basic sizes.



where,

$f_0$ : Resonance frequency,  $L$ : Equivalent inductance,

$C$ : Equivalent capacitance,  $R$ : Equivalent resistance,

$Q$ : Quality factor,

$C_0$ : Equivalent capacity of spring element as preload to vaneplate,

$k_0$ : Spring constant of spring element,  $A$ : Force factor.

Fig. 2. Equivalent circuit of stator vibrator with preload to vaneplate at resonance and relational expressions.

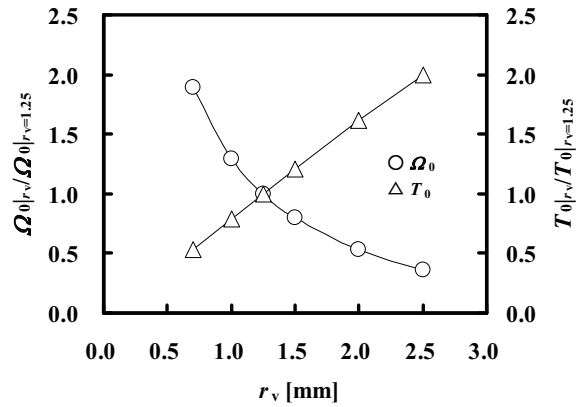


Fig. 5.  $r_v$  dependence of revolution speed and torque for motor.



Fig. 6. Overviews of cantilever-type motor and stator with  $r_v = 4$  mm: (a) motor rotor with CD-R shaped rotor, (b) stator vibrator.